Chirality transfer in nematic liquid crystals doped with (*S*)-naproxen-functionalized gold nanoclusters: an induced circular dichroism study†

Hao Qi, Joe O'Neil and Torsten Hegmann*

Received 16th August 2007, Accepted 9th November 2007
First published as an Advance Article on the web 4th December 2007
DOI: 10.1039/b712616f

In a recent study, we found that nematic liquid crystals (N-LCs) doped with chiral (*S*)-naproxen-functionalized dodecane thiolate protected gold nanoclusters (**Au2**, **Au3**) or non-chiral alkyl thiolate protected Au clusters (**Au1**) produce thin film textures with characteristic uniform stripe patterns separated by areas of homeotropic alignment. While these textures closely resemble textures commonly observed for chiral nematic (N*-)phases with large helical pitch, so-called cholesteric finger textures, they originate from local concentration differences of the nanoclusters in the N-LC solvent. While areas with higher particle content form linear particle aggregates (stripe domains) due to the surface anchoring of the N-LC molecules to the cluster surface, areas of lower particle concentration give homeotropic alignment as a result of particles residing at the glass–N-LC interfaces. To elucidate and confirm a chirality transfer from the chirally modified gold clusters to the non-chiral N-LC, despite the complex thin film textures, we here present detailed induced circular dichroism (ICD) studies of thin films of 5CB doped with the three different Au clusters. These experiments revealed that the chiral Au nanoclusters (**Au2**, **Au3**) successfully transfer chirality to the N-LC host producing a chiral nematic phase (N*) with the opposite helical sense in comparison to the pure, organic chiral dopant dispersed in the same N-LC host. Thus, these results provide the first experimental proof for the usefulness of gold nanoclusters as chiral dopants for N-LCs. In contrast, for the non-chiral Au cluster, at a macroscopic level, no relationship between the cholesteric finger-like textures and chirality was found.

Introduction

Optically active (chiral) materials can be classified into two classes: intrinsically chiral materials (on a molecular level) and extrinsically chiral materials. Extrinsically chiral materials are based on a chiral molecular organization, which does not require chiral constituents or molecules.[1] In N-LCs (as well as tilted smectic LCs), induced circular dichroism (ICD) is the extrinsic circular dichroism due to the helical arrangement of the molecules. There are two main types of ICD: the first type includes chiral LCs doped with non-chiral molecules showing CD signals at the absorption wavelength of the non-chiral dopant molecules due to the induced helical arrangement through interactions with the LC (mimicking the helical organization),[2] and the second type includes chiral LC phases induced by a chiral dopant[3] (or mechanically induced by using a twisted cell) showing CD signals at the LC host absorption band.[4] Both types of ICD have been widely studied over the past several years.[1,4–10]

Two main textures can be found for N*-LCs using alignment layers: focal conic fingerprint texture, with the helical axes parallel to the surface, and Grandjean (planar) texture, with the helical axes perpendicular to the surface.[11] The focal conic texture shows birefringence but is optically inactive, whereas the Grandjean texture exhibits optical effects of the chiral mesophase and is suitable for CD measurements.[12,13] One of the most interesting properties related to the Grandjean texture is the selective reflection of circularly polarized light at a wavelength commensurate with the helical pitch by the equation $\lambda = np$, where n is the mean refractive index, and p is the helical pitch.[14] The reflection is related to the handedness, *i.e.* right-handed N*-LCs only reflect right-circularly polarized light and show no effect on left-circularly polarized light, and *vice versa* for left-handed N*-LCs.[14] As a result, both a circular reflection band and a circular adsorption band can be measured as a result of the chirality of the N*-LCs.[5] In some cases, a decreasing ICD intensity was observed during the transformation of the Grandjean texture into a focal conic fingerprint texture.[8,14] Without surface alignment or other special treatment, N*-LCs commonly form multi-domains, and a signal in the CD-spectra related to selective reflection can be observed even in the absence of a planar texture. Additionally, the CD-band shape in these cases is commonly quite broad indicating the random distribution of the chiral domains.[15] In the absorption region, the apparent CD signal is a combination of the real CD signal, linear dichroism (LD), and birefringence. LD and birefringence effects, however, can be cancelled out by rotating the cell through 360° normal to the incident light beam.[16,17] In similar experiments, aside from the described optical characteristics (textures) of N*-LC phase, CD spectropolarimetry has shown to be a powerful technique

Department of Chemistry, University of Manitoba, Winnipeg, Manitoba, R3T 2N2 Canada. E-mail: hegmannt@cc.umanitoba.ca; Fax: 1 (204) 474 7608; Tel: 1 (204) 474 7535

† Electronic supplementary information (ESI) available: POM micrographs of the N- or N*-phases at room temperature after cooling from the isotropic liquid phase at a cooling rate of 1 °C min^{-1}; UV-vis absorption and CD spectra. See DOI: 10.1039/b712616f

 This journal is © The Royal Society of Chemistry 2008

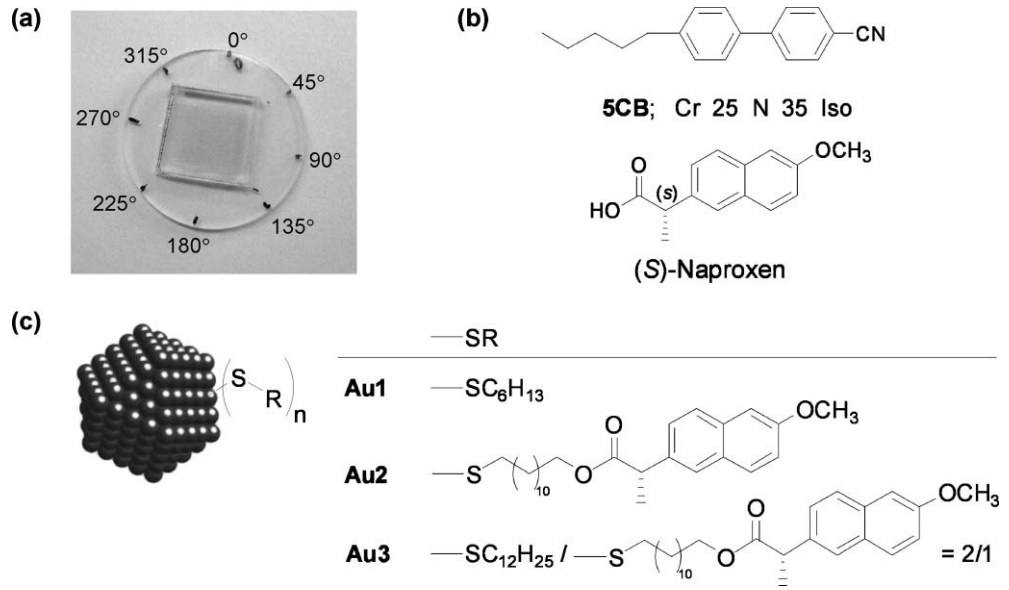

Fig. 1 (a) Photo of prepared sample; (b) structure and phase transition temperature (°C) of 5CB and (*S*)-naproxen. Cr = crystalline solid, N = nematic phase and Iso = isotropic phase; (c) gold nanoclusters and structure of thiolate protecting agents (*n* = number of thiolates coating the nanocluster; *n* depends on the nanocluster size).

to prove LC phase chirality, and has successfully been utilized for chiral nematic (N*), chiral smectic-C (SmC*), and bent-core (bow or banana-shaped) LC phases.[1–26]

In an attempt to combine the unique size-dependent properties of nanoscale materials and chirality by creating chirally decorated gold nanoclusters as dopants for N-LCs, we have recently shown that N-LCs upon doping with chiral (*S*)-naproxen-functionalized alkyl thiolate coated gold clusters produce thin film textures characterized by periodic stripe domains separated by dark areas showing no birefringence. These textural characteristics closely resemble textures commonly observed for N*-phases with large helical pitch, termed cholesteric finger textures.[11] Surprisingly, the same texture was also found for mixtures containing non-chiral dodecane or hexane thiolate protected Au clusters.[27]

Considering the strong homeotropic anchoring of the N-LC molecules to the nanocluster surface (dispersion, van der Waals interactions), the formation of linear particle aggregates as a result of the formation of topological defects (dipole, and hyperbolic hedgehog), and particles residing at the glass–N-LC interfaces producing homeotropic alignment in the domains separating the stripes were discussed as the main driving forces for this texture formation. At that point, we were unable to confirm whether the chiral Au nanoclusters transfer chirality to N-LCs, or not, solely based on the texture. In addition, given the formation of the described defects we were unable to produce uniform aligned samples between polyimide-coated glass slides (LC test cells with polyimide alignment layers) for these N-LC/nanocluster mixtures,[27] making it impossible to use non-spectroscopic methods such as the Grandjean–Cano technique[28] or the Cano wedge method[29] to measure the helical pitch.

To provide experimental evidence for a chirality transfer (induction) in the N-LC–gold nanocluster mixtures, and to study the differences between N-LC–chiral Au cluster (gold nanocluster chiral dopants) and N-LC–non-chiral Au cluster mixtures, we here present detailed induced circular dichroism (CD) studies of thin films of a N-LC (5CB) doped with Au nanoclusters. Thin films of 5CB doped with the three different Au nanoclusters (one non-chiral: **Au1**, and two chiral; **Au2** and **Au3**) were first observed by polarized optical microscopy (POM), and characterized by UV-vis absorption, followed by ICD spectroscopy.

Experimental

Details of the synthesis of the gold nanoclusters, their characterization, and preparation of the mixtures with N-LCs were reported previously.[27] In this study, we use 5CB as the host LC, as 5CB shows a N phase at room temperature, which is convenient for CD measurements. The structures of 5CB, (*S*)-naproxen and the gold nanoclusters used are shown in Fig. 1. Thin films of 5CB–**Au1**–**Au3** mixtures were prepared as follows. One quartz plate and one smaller square quartz plate were separated by Mylar spacers of a nominal thickness of 12 μm‡, and epoxied at four points [Fig. 1(a)].[30] These cells were then filled with the mixtures at a temperature above the clearing point of 5CB (*ca.* 40 °C), and then slowly cooled down to the N phase at a cooling rate of 1 °C min^{-1}. CD spectra were recorded on a J-810 spectropolarimeter (Jasco, Inc.) using a bandwidth of 2 nm, medium sensitivity with a maximum of 200 mdeg (except for specifically indicated samples). During the CD measurement, each cell was rotated normal to the light

‡ Minor variations in cell thickness, due to the preparation of the sandwiched quartz cells using Mylar spacers and epoxy, cannot be excluded. The resulting variations in the LC film thickness will contribute to a difference in signal intensity. While this could likely have been avoided to some degree by using a room temperature LC mixture with lower aromatic content, contributions of linear dichroism and birefringence, particularly for mixtures with lower particle content, seem to play a more critical role (although they do not affect the observed sign of the CD signal).

beam in 45° intervals from 0° to 315° to differentiate the intrinsic CD from linear dichroism and birefringence. UV-vis absorption spectra were measured using a Cary 5000 UV-vis-NIR spectrophotometer (Varian), and POM was performed using an Olympus BX51-P polarizing microscope in conjunction with a Linkam LS350 heating/cooling stage.

Results and discussion

Pure 5CB and 5CB doped with (*S*)-naproxen were both tested first allowing us to compare the obtained CD spectra with the spectra of the 5CB–Au nanocluster mixtures. As observed by POM, the pure 5CB cell shows a typical nematic marble texture as shown in the ESI (Fig. S1a).† Absorbance and CD spectra of 5CB are also collected in the ESI [Fig. S2(a) and (b)].† 5CB shows two absorption peaks at 200 and 280 nm, respectively.[31] However, the LC film must be very thin to display a real peak without saturation of the detector. For example, in a paper published by Hird and co-workers,[31] suitable thin films of 5CB with 0.2–0.4 μm nominal thickness prepared using pulsed laser deposition show the related 280 nm absorption peak. As demonstrated by Hird and co-workers, a typical LC texture cannot be observed with such thin films.[31]

In the present study, we did not attempt to produce sub-micron thin films showing no characteristic textures, since we were focusing on measuring the CD spectra of the binary N-LC–Au nanocluster mixtures showing the described textures that would allow us to examine possible relationships between the two components and the potential of inducing chirality. However, due to the thickness of these films, the absorbance is quite strong resulting in a saturation of the absorbance up to 318 nm. Therefore, only the edge above 318 nm of the 280 nm absorbance peak is shown in all CD spectra (real signal), and used in the discussion of induced chirality from the various dopants to the N-LC. This also applies to the 0° CD spectrum in Fig. S2b shown in the ESI (included for comparison).†

CD spectroscopy measures the difference in absorbance of left- and right-handed circularly polarized light by a given specimen. In the presented experiments, if the absorbance is saturated due to the film's thickness, the zero CD signal in the saturated part of the spectrum below 320 nm only means that there is no light passing through the cell. The CD signal is saturated up to *ca.* 320 nm and decreases to zero at shorter wavelengths due to the saturated absorbance. In effect, only the edge shown in all spectra should be regarded as a true CD signal. For the same reason, not the intensity but the sign of the CD signals is discussed and related to chirality, as pointed out by Green *et al.*[9] As expected for pure, non-chiral 5CB (see ESI†), rotating the cell produced CD spectra showing regularly positive or negative signals due to linear dichroism and birefringence.

To measure a true CD of the N*-phase formed by doping a chiral dopant such as (*S*)-naproxen into a non-chiral N phase, we first need to know whether the CD signal is due to the induced chiral arrangement of the N-LC host, or due to the dopant's absorption itself. To exclude this, sub-micron thin films of pure 5CB and 5CB doped with 0.1 wt% (*S*)-naproxen were prepared by drop-casting solutions on one quartz plate, followed by evaporation of the solvent, heating the samples above the clearing point, and subsequent cooling to room temperature. The two UV-vis absorption spectra (see ESI†) are quite similar, both showing an absorption maximum at 280 nm for 5CB indicating only a very minor contribution from (*S*)-naproxen to the spectrum. Hence, all CD spectra of the 12 μm thick films are showing signals with the major contribution arising from 5CB as the chromophore. Similarly, the absorption spectra of 12 μm thick cells of 5CB doped with both 0.1 wt% and 0.01 wt% (*S*)-naproxen are almost identical to the spectrum of pure 5CB (ESI†) with minor differences in absorbance at longer wavelengths starting at 330 nm (both spectra are saturated below 320 nm).

Another point one has to take into consideration is that only low concentrations of a chiral dopant can be used. As can be seen from the CD spectrum of 5CB doped with 0.1 wt% (*S*)-naproxen (ESI†), higher chiral dopant concentrations produce stronger CD reflection signals out of the measurable range of the CD instrument [even at low sensitivity no changes in the spectral shape are apparent (maximum 2000 mdeg)]. Similar to the experiments described by Harkness and Gray using unmodified surfaces,[15] the reflection band is quite broad as a result of multi-domain formation. However, a tenfold decrease in the (*S*)-naproxen concentration (0.01 wt%) produces a CD spectrum with the edge at a longer wavelength (red color in Fig. S2d in ESI†) considered to be the real part of the CD signal. Between 350 and 330 nm, the negative CD signal arises from the selective reflection of the induced N*-phase. At shorter wavelengths starting at *ca.* 330 nm, the observed increasing negative intensity of the CD spectrum is related to the absorption, which is further modified by contributions of the linear dichroism and birefringence. As expected for an N*-phase, rotating the sample did not change the shape and the sign of the CD-band.

While it seems logical to assume that Au nanoclusters decorated with the same enantiomerically-enriched chiral dopant moiety [*i.e.* (*S*)-naproxen] would serve as chiral dopants for LC phases inducing an N*-phase with the same handedness, the unexpected similarity of the textures for both (*S*)-naproxen decorated Au clusters (**Au2**, **Au3**) and hexane thiolate (**Au1**) and dodecane thiolate protected Au nanoclusters warranted caution in making this conclusion simply based on textural observations. In addition, a bulk chiral induction in a N-phase by a minute amount of chirally decorated gold nanoclusters (5 wt% ~ 0.04 mole% depending on the nanocluster size) would provide evidence that nanoclusters in the few-nanometre size regime can influence or change the nematic environment on a macroscopic level, and are therefore not "invisible" to the N-LC host.

Depending on the LC host structure and the Au nanocluster concentration, fingerprint-like or cholesteric finger-like textures can be observed, or birefringent stripes can co-exist beside domains displaying non-chiral nematic schlieren textures. The commonly observed texture with stripe domains resulting from linear particle aggregates of 5CB doped with 5 wt% **Au2** is shown in Fig. 2(a). For 5CB doped with the nanoclusters, further cooling at higher cooling rates, or lower particle concentrations, sometimes produces 'normal' schlieren textures, which are not indicative of an N*-phase. For example, reducing the concentration of **Au2** to 1 wt%

 This journal is © The Royal Society of Chemistry 2008

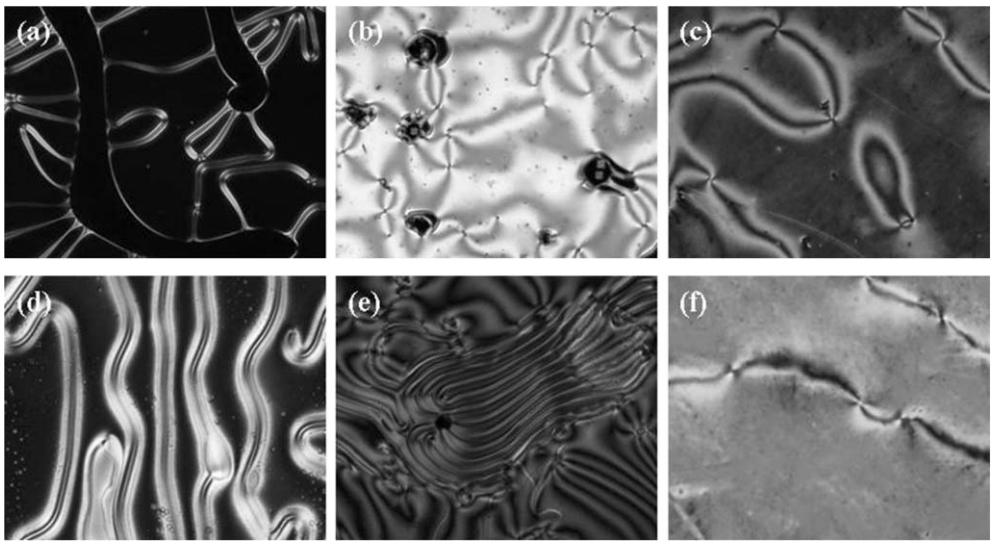

Fig. 2 POM micrographs of (a) 5CB doped with 5 wt% **Au2** at the transition from the isotropic liquid to the N*-LC phase (34.6 °C), (b) 5CB doped with 5 wt% **Au2** at room temperature, (c) 5CB doped with 1 wt% **Au2** at room temperature, (d) 5CB doped with 5 wt% **Au3** at 33.9 °C on cooling, (e) 5CB doped with 5 wt% **Au3** at room temperature, and (f) 5CB doped with 0.5 wt% **Au3** at room temperature.

produced schlieren textures as shown in Fig. 2(c). However, despite the formation of a typical non-chiral schlieren texture for the 5CB–**Au2** mixture, the CD absorption spectra [Fig. 3(a) and (b)] clearly show the chirality of the system. As can be seen from Fig. 3(b), although there are obvious linear dichroism and birefringence effects on the apparent CD signal, always positive CD signals for all sample rotation angles were observed, although the intensity at different angles varies, and provides clear evidence for induced chirality from the chiral gold nanocluster to the N-LC host. This result is distinctly different from the CD spectra obtained for 5CB doped with (*S*)-naproxen (see ESI†), for which all CD-bands showed a negative sign. For 5CB doped with 5 wt% **Au2**, a higher concentration of chiral (*S*)-naproxen units (higher intensity in the CD spectra) reduces the relative contribution of linear dichroism and birefringence; the negative sign and the intensity of the CD signal are again independent of rotation angle. Aside from the lack of a clear CD reflection signal in the 5CB–**Au2** spectra, which is likely the result of a larger helical pitch of the 5CB–**Au2** mixture because of the overall lower concentration of (*S*)-naproxen (concentration-dependent helical pitch), the difference in sign was found to be the major difference between the CD spectra of 5CB–**Au2** and 5CB doped 0.1 wt% or 0.01 wt% (*S*)-naproxen.

Similar results were also obtained for mixtures of 5CB doped with **Au3**. Fig. 2(d) and (e) show the textures of 5CB doped with 5 wt% **Au3**. Likely due to the smaller size of **Au3** (1.4 nm for **Au3** *vs.* 3.5 nm for **Au2**), slightly different textural characteristics are observed. Upon cooling from the isotropic liquid phase, 5CB doped with **Au3** initially formed birefringent stripes separated by homeotropic domains that turn into schlieren texture domains at room temperature. Similar to 5CB doped with (*S*)-naproxen, 5CB doped with 5 wt% **Au3** displays a strong CD reflection signal out of the measurable range of the CD instrument. Most importantly, the real part of the CD spectrum (edge) has again a positive sign for each rotation angle. This is also true for the same mixture with lower **Au3** content (0.5 wt% **Au3**) showing a typical schlieren texture by POM because of the lower particle concentration. These results support our assumption that the chirally decorated gold nanoclusters transfer chirality to the N-LC host. Similar to the CD spectra of the pure, isolated gold nanoclusters **Au2** and **Au3** in comparison to the CD spectrum of pure (*S*)-naproxen,[27] 5CB doped with (*S*)-naproxen produces negative CD signals, and 5CB–**Au2** and 5CB–**Au3** constantly positive signals at all measured sample rotation angles [Figs. 3(c) and (d)]. This sign reversal must then be the result of a reverse rotation of N-LC molecules in these two systems, one left- and one right-handed. Such variation in chirality from the free (*S*)-naproxen to (*S*)-naproxen moieties tethered to the gold nanocluster surface *via* hydrocarbon chains can be expected, and related effects have previously been reported for side-chain LC polymers.[32] In fact, chiral inversions in nematic and smectic-C liquid crystals are a common phenomenon, and have been reported by a number of groups.[33]

While it seems impossible, because of size and local (*S*)-naproxen concentration differences, to quantify the propensity of **Au2** and **Au3** to induce chirality in the N-LC host based on texture observations and CD spectra, a clear trend can be observed. As for commonly used organic chiral dopants, a higher concentration of **Au2** or **Au3** in 5CB results in a shorter helical pitch,[34] and more intense CD signals are observed as a result thereof. Relevant factors such as the impossibility to obtain homogenous planar textures for the chirally decorated clusters along with the larger film thickness make it impossible to measure perfect CD reflection and absorption spectra. However, from the edge of the CD absorption and broad reflection spectra (here only **Au3**) we can conclude that **Au2** and **Au3** successfully transfer chirality to the non-chiral N-LC host with the opposite helical sense as the pure, organic chiral dopant in the same N-LC.[32,33]

The last step was to study the finger-like texture formed by 5CB doped with hexane thiolate protected Au nanoclusters (**Au1**). The chirality of Au nanoclusters is still an open

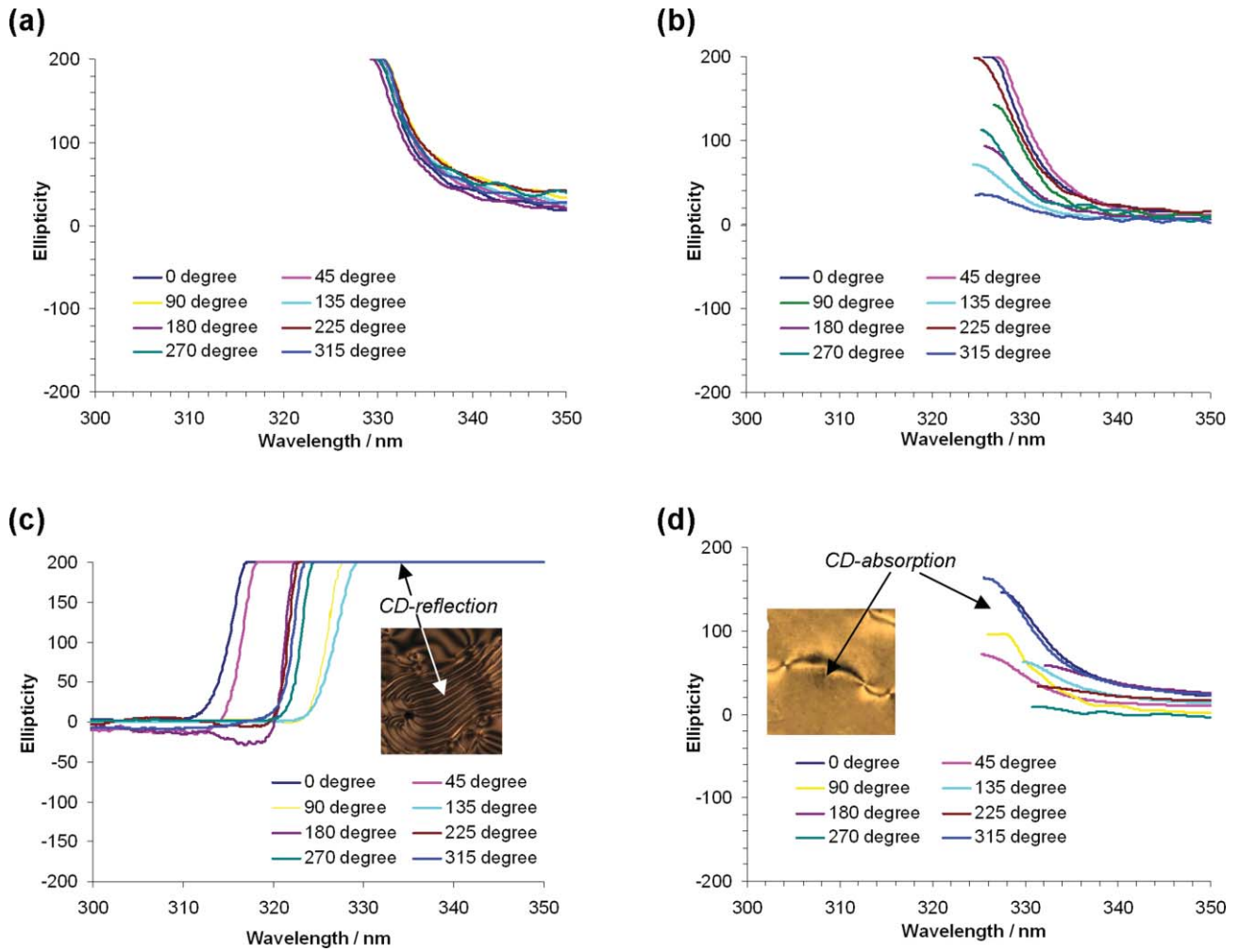

Fig. 3 CD spectra at different sample angular rotation angles of (a) 5CB doped with 5 wt% **Au2**, (b) 5CB doped 1 wt% **Au2,** (c) 5CB doped with 5 wt% **Au3**, and (d) 5CB doped with 0.5 wt% **Au3**.‡

question.[35] The existence of local chirality of related silver nanoparticle aggregates, which can be regarded as a racemic mixture at the macroscopic level, was recently proposed by Drachev *et al.* using experiments such as photon scanning tunneling microscopy.[36] Although theoretical studies point out that the most stable isomers of bare Au_{28}, Au_{55}, and thiolate protected gold clusters can be chiral,[37–41] no related experimental results proving chiral or macroscopic racemic properties of bare or non-chiral, thiol-protected Au nanoclusters *via* a chirality transfer and 'amplification' in a condensed phase have been reported so far.

To clarify the origin of the textural similarities (linear particle aggregates) we observed for chiral and non-chiral modified gold nanoclusters, and their relationship to possible local or macroscopic chirality of the N-LC mixtures, we further studied ICD of thin films of 5CB doped with **Au1**.

Fig. 4(a) shows the texture of 5CB doped with 1 wt% **Au1** at the transition from the isotropic liquid phase to the nematic phase on cooling, which appears quite similar to textures observed for **Au2** and **Au3** in 5CB shown in Fig. 2(a) and (d). With a slow cooling rate (<1 °C/min), even though most stripes disappear upon further cooling, several birefringent

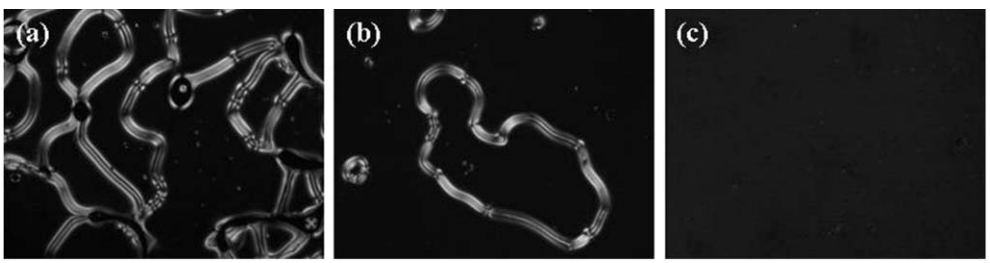

Fig. 4 POM micrograph of 5CB doped with 1 wt% **Au1**: (a) at 33.4 °C, (b) at room temperature (slow cooling), and (c) at room temperature showing no-stripes after rapid cooling.

 This journal is © The Royal Society of Chemistry 2008

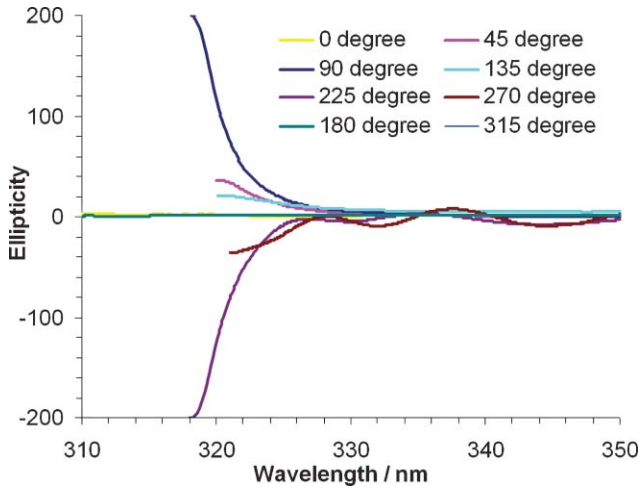

Fig. 5 CD spectra of 5CB doped with 1 wt% **Au1** showing birefringent stripes at different sample rotation angles.‡

stripes remain clearly visible [Fig. 4(b)] at room temperature. In contrast, for faster cooling rates (achieved by opening the cover of the heating stage to increase the cooling rate), in some cases, all stripes disappear for the **Au1** clusters in 5CB, and exclusively homeotropic alignment of the N-LC molecules is obtained [Fig. 4(c)]. These are excellent samples to study eventual chiral effects in these mixtures (related to the stripes or not). For the 5CB–1 wt% **Au1** mixture with roughly the same or higher area density of stripes as observed for **Au3** in 5CB, if the stripes are a result of local chirality, *i.e.* the alignment or orientation of the N-LC molecules adopts a helical arrangement, a constant positive or negative sign of the CD spectra will not be affected by rotating the sample about different sample rotation angles. The homeotropic domains as shown in Fig. 4(b), and the homeotropically aligned film in Fig. 4(c) should not give rise to any CD signal. The CD spectra of 5CB doped with 1 wt% **Au1** with birefringent stripe domains [linear particle aggregates as in Fig. 4(a) and (b)] is shown in Fig. 5.

One can clearly see that the CD signal shows either negative or positive signs at different sample rotation angles, with several angles showing no (0°, 180°) or very weak CD signals (315°) (zero ellipticity). The similarity of these CD spectra with the CD spectra obtained for pure 5CB clearly demonstrates that there is no macroscopic chirality associated with the birefringent stripes. As expected then, the spectra of the complete homeotropically aligned film did not show any CD signal for any rotation angle (not shown). Based on these measurements, although local chiral distortions or a twist in the director configuration can not be completely excluded (since the birefringent stripes remain visibly colored even with uncrossed (parallel) polarizers[27], macroscopically no chirality is induced in the non-chiral N-phase by 'simple' alkyl thiolate capped gold nanoclusters.

Conclusions

To summarize, ICD measurements of 5CB doped with chiral Au nanoclusters (**Au2**, **Au3**) prove the successful transfer of chirality from the chirally capped Au nanoclusters to the non-chiral nematic LCs with a sign inversion (opposite helical sense)[32,33,42] from the pure, organic chiral dopant to chiral dopant decorated Au nanoclusters. To the best of our knowledge, this is the first example of induced LC chirality by Au nanoparticles. As nematic LCs doped with chiral additives are widely used in liquid crystal display (LCD) technologies, we foresee the possibility of using chiral Au nanoclusters in such and related applications by combining the chiral dopant capabilities reported here with the unique size and shape-dependent properties of alkylthiol capped nanoscale gold clusters such as, optical and electronic properties,[43] room temperature magnetism,[44] or luminescent blinking.[45] In addition, gold nanoparticle–N-LC mixtures were used for electrically controlled light scattering (near-field spectral tuning),[46] a proof-of-concept device capable of voltage-dependent color tuning (far-field spectral tuning),[47] and nematic mixtures with higher conductivity.[48]

Finally, we have also shown that alkyl thiolate protected gold nanoclusters, despite similar textural effects in N-LCs, and theoretical as well as experimental indications of chirality of bare and thiolate protected metal (Au, Ag) nanoclusters, do not give rise to macroscopically detectable chiral effects, conformations, or aggregates in N-LCs.

Acknowledgements

This work was supported by the Natural Sciences and Engineering Research Council (NSERC) of Canada, the Canada Foundation for Innovation (CFI), the Manitoba Research and Innovations Fund (MRIF), and the University of Manitoba (Demonstration Project Grant).

References

1 F. D. Saeva, in *Liquid Crystals, the Fourth State of Matter*, ed. F. D. Saeva, Marcel Dekker, New York, 1979, pp. 249–273.
2 F. D. Saeva and J. J. Wysocki, *J. Am. Chem. Soc.*, 1971, **93**, 5928–5929.
3 For an overview see: (*a*) *Chirality in Liquid Crystals (Partially Ordered Systems)*, ed. H.-S. Kitzerov and C. Bahr, Springer, Heidelberg, 2001; (*b*) G. Solladie and R. G. Zimmermann, *Angew. Chem., Int. Ed. Engl.*, 1984, **23**, 348–362.
4 F. D. Saeva, *Mol. Cryst. Liq. Cryst.*, 1973, **23**, 171–177.
5 G. P. Spada and G. Proni, *Enantiomer*, 1998, **3**, 301–314.
6 F. D. Saeva, *J. Am. Chem. Soc.*, 1972, **94**, 5135–5136.
7 J. Lee, Y. Ouchi, H. Takeze, A. Fukuda and J. Watanabe, *J. Phys.: Condens. Matter*, 1990, **2**, 271–274.
8 X. M. Dong and D. G. Gray, *Langmuir*, 1997, **13**, 3029–3034.
9 A similar situation was discussed by Green *et al*. In their paper, because of the strong optical density of the sample, only the CD at the absorbance band edge was measured; M. M. Green, S. Zanella, H. Gu, T. Sato, G. Gottarelli, S. K. Jha, G. P. Spada, A. M. Schoevaars, B. Feringa and A. Teramoto, *J. Am. Chem. Soc.*, 1998, **120**, 9810–9817.
10 S. Fireman-Shoresh, S. Marx and D. Avnir, *J. Mater. Chem.*, 2007, **17**, 536–544.
11 I. Dierking, *Textures of Liquid Crystals*, Wiley-VCH, Weinheim, 2003, pp. 51–70.
12 H. W. Gibson, in *Liquid Crystals, the Fourth State of Matter*, ed. F. D. Saeva, Marcel Dekker, New York, 1979, pp. 99–162.
13 G. Gottarelli and G. P. Spada, in *Circular Dichroism – Principles and Applications*, ed. K. Nakanishi, N. Berova and R. W. Woody, VCH, New York, 1994, pp. 547–561.
14 F. D. Saeva, P. E. Sharpe and G. R. Olin, *J. Am. Chem. Soc.*, 1973, **95**, 7656–7659.

15 B. R. Harkness and D. G. Gray, *Macromolecules*, 1991, **24**, 1800–1805.
16 F. D. Saeva and G. R. Olin, *J. Am. Chem. Soc.*, 1976, **98**, 2709–2711.
17 C. Spitz, S. Dahne, A. Ouart and H. W. Abraham, *J. Phys. Chem. B*, 2000, **104**, 8664–8669.
18 J. M. Ribo, J. Crusats, F. Sagues, J. Claret and R. Rubire, *Science*, 2001, **292**, 2063–2066.
19 J. Yuan and M. Liu, *J. Am. Chem. Soc.*, 2003, **125**, 5051–5056.
20 S.-W. Choi, S. Kang, Y. Takanishi, K. Ishikawa, J. Watanabe and H. Takezoe, *Angew. Chem., Int. Ed.*, 2006, **45**, 6503–6506.
21 D. Katsis, P. H. M. Chen, J. C. Mastrangelo and S. H. Chen, *Chem. Mater.*, 1999, **11**, 1590–1598.
22 J. Yoshida, H. Sato, A. Yamagishi and N. Hoshimo, *J. Am. Chem. Soc.*, 2005, **127**, 8453–8456.
23 Y. Takanishi, G. J. Shin, J. C. Jung, S.-W. Choi, K. Ishiwawa, J. Watanabe, H. Takezoe and P. Toledano, *J. Mater. Chem.*, 2005, **15**, 4020–4024.
24 N. Hoshino, Y. Matsuoka, K. Okamoto and A. Yamagishi, *J. Am. Chem. Soc.*, 2003, **125**, 1718–1719.
25 T. Mitsuoka, H. Sato, J. Yoshida, A. Yamagishi and Y. Einaga, *Chem. Mater.*, 2006, **18**, 3442–3447.
26 C. Nuckolls and T. J. Kata, *J. Am. Chem. Soc.*, 1998, **120**, 9541–9544.
27 H. Qi and T. Hegmann, *J. Mater. Chem.*, 2006, **16**, 4197–4205.
28 (*a*) F. Grandjean, *C. R. Hebd. Seances Acad. Sci.*, 1921, **172**, 71–74; (*b*) R. Cano, *Bull. Soc. Fr. Mineral.*, 1968, **91**, 20–27; (*c*) G. Heppke and F. Oestreicher, *Mol. Cryst. Liq. Cryst.*, 1978, **41**, 245–249.
29 (*a*) G. Gottarelli, B. Samori, C. Stremmenos and G. Torre, *Tetrahedron*, 1981, **37**, 395–399; (*b*) For an illustration of the Cano wedge method see: K. Akagi, S. Guo, T. Mori, M. Goh, G. Piao and M. Kyotani, *J. Am. Chem. Soc.*, 2005, **127**, 14647–14654.
30 J. F. Li, K. A. Crandall, P. W. Chu, V. Percec, R. G. Petschek and C. Rosenblatt, *Macromolecules*, 1996, **29**, 7813–7819.
31 J. Gonzalo, P. E. Dyer and M. Hird, *Appl. Phys. Lett.*, 1997, **71**, 2752–2754, and references cited therein.
32 For effects in chiral LC polymers (side-chain and main-chain) and chiral LC polymer mixtures see: (*a*) M. Goh, T. Matsushita, M. Kyotani and K. Akagi, *Macromolecules*, 2007, **40**, 4762–4771; (*b*) D. B. Amabilino, J. L. Serrano, T. Sierra and J. Veciana, *J. Polym. Sci., Part A: Polym. Chem.*, 2006, **44**, 3161–3174; (*c*) M. M. Green and C. Khatri, *Macromol. Symp.*, 1994, **77**, 277–282; (*d*) I. Rusig, M. H. Godinho, L. Varichon, P. Sixou, J. Dedier, C. Filliatre and A. F. Martins, *J. Polym. Sci., Part B: Polym. Phys.*, 1994, **32**, 1907–1914; (*e*) V. Percec and M. Kawasumi, *Macromolecules*, 1993, **26**, 3917–3928; (*f*) J. C. Mastrangelo and S. H. Chen, *Macromolecules*, 1993, **26**, 6132–6134; (*g*) R. A. Lewthwaite, J. W. Goodby and K. J. Toyne, *J. Mater. Chem.*, 1993, **3**, 241–245; (*h*) M. Radianguenebaud and P. Sixou, *Mol. Cryst. Liq. Cryst.*, 1992, **220**, 53–62; (*i*) P. Sixou, J. M. Gilli, A. Tenbosch, F. Fried, P. Maissa, L. Varichon and M. H. Godinho, *Phys. Scr.*, 1991, **35**, 47–52; (*j*) L. Varichon, A. Tenbosch and P. Sixou, *Liq. Cryst.*, 1991, **9**, 701–709; (*k*) J. M. G. Cowie and H. W. Hunter, *Macromol. Chem. Phys.*, 1991, **192**, 143–151.
33 For examples of chirality inversion in LC phases see: (*a*) C. Y. Li, S. Jin, X. Weng, J. J. Ge, D. Zhang, F. Bai, F. W. Harris, S. Z. D. Cheng, D. H. Yan, T. B. He, B. Lotz and L. C. Chien, *Macromolecules*, 2002, **35**, 5475–5482; (*b*) B. P. Huff, J. J. Krich and P. J. Collings, *Phys. Rev. E*, 2000, **61**, 5372–5378; (*c*) A. V. Emelyanenko, M. A. Osipov and D. A. Dunmur, *Phys. Rev. E*, 2000, **62**, 2340–2352; (*d*) D. J. Photinos and E. T. Samulski, *Science*, 1995, **270**, 783–786; (*e*) I. Dierking, F. Giesselmann, P. Zugenmaier, K. Mohr, H. Zaschke and W. Kuczynski, *Z. Naturforsch., A*, 1994, **49**, 1081–1086; (*f*) K. Radley and N. McLay, *J. Phys. Chem.*, 1994, **98**, 3071–3072; (*g*) P. Styring, J. D. Vuijk, I. Nishiyama, A. J. Slaney and J. W. Goodby, *J. Mater. Chem.*, 1993, **3**, 399–405; (*h*) A. J. Slaney, I. Nishiyama, P. Styring and J. W. Goodby, *J. Mater. Chem.*, 1992, **2**, 805–810.
34 D. J. Broer and I. Heynderickx, *Macromolecules*, 1990, **23**, 2474–2477.
35 M. Bieri, C. Gautier and T. Burgi, *Phys. Chem. Chem. Phys.*, 2007, **9**, 671–685.
36 V. P. Drachev, W. D. Bragg, V. A. Podolskiy, V. P. Safonov, W. T. Kim, Z. C. Ying, R. L. Armstrong and V. M. Shalaev, *J. Opt. Soc. Am. B*, 2001, **18**, 1896–1903.
37 I. L. Garzón, J. A. Reyes-Nave, J. I. Rodriguez-Hernández, I. Sigal, M. R. Beltrán and K. Michaelian, *Phys. Rev. B: Condens. Matter*, 2002, **66**, 0734031–4.
38 I. L. Garzón, M. R. Beltrán, G. González, I. Gutierrez-González, K. Michaelian, J. A. Reyes-Nava and J. I. Rodriguez-Hernández, *Eur. Phys. J. D*, 2003, **24**, 105–109.
39 C. E. Román-Velázques, C. Noguez and I. L. Garzón, *J. Phys. Chem. B*, 2003, **107**, 12035–12038.
40 X. López-Lozano, L. A. Pérez and I. L. Garzón, *Phys. Rev. Lett.*, 2006, **97**, 233401.
41 A. Lechtken, D. Schooss, J. R. Stairs, M. N. Blom, F. Furche, N. Morgner, O. Kostko, B. V. Issendorff and M. M. Kappes, *Angew. Chem., Int. Ed.*, 2007, **46**, 2944–2948.
42 A related effect was reported for dendrimers with a chiral periphery: J. F. G. A. Jansen, H. W. I. Peerlings, E. M. M. de Brabander van den Berg and E. W. Meijer, *Angew. Chem., Int. Ed. Engl.*, 1995, **34**, 1206–1209.
43 (*a*) M. Brust, *Nat. Mater.*, 2005, **4**, 364–365; (*b*) A. C. Templeton, W. P. Wuelfing and R. W. Murray, *Acc. Chem. Res.*, 2000, **33**, 27–36.
44 (*a*) J. de la Venta, A. Pucci, E. Fernández Pinel, M. A. García, F. de Julián, P. Crespo, P. Mazzoldi, G. Ruggeri and A. Hernando, *Adv. Mater.*, 2007, **19**, 875–877; (*b*) Y. Yamamoto and H. Hori, *Rev. Adv. Mater. Sci.*, 2006, **12**, 23–32.
45 C. D. Geddes, A. Parfenov, I. Gryczynski and J. R. Lakowicz, *Chem. Phys. Lett.*, 2003, **380**, 269–272.
46 J. Müller, C. Sönnichsen, H. von Poschinger, G. von Plessen, T. A. Klar and J. Feldmann, *Appl. Phys. Lett.*, 2002, **81**, 171–173.
47 P. A. Kossyrev, A. Yin, S. G. Cloutier, D. A. Cardimona, H. Danhong, P. M. Alsing and J. M. Xu, *Nano Lett.*, 2005, **5**, 1978–1981.
48 S. K. Prasad, K. L. Sandhya, G. G. Nair, U. S. Hiremath, C. V. Yelamaggad and S. Sampath, *Liq. Cryst.*, 2006, **33**, 1121–1125.

 This journal is © The Royal Society of Chemistry 2008